computing@tanet.edu.te.ua
www.tanet.edu.te.ua/computing

ISSN 1727-6209
International Scientific Journal of Computing

COLORED LIGHT-TO-VOLTAGE CONVERTERS BASED ABSORBANCE METER

M. Pereira[1], O. Postolache[1,2], P. Girão[2], Helena Ramos[2]

1.Escola Superior de Tecnologia de Setúbal, Instituto Politécnico de Setúbal, 2914-508 Setúbal, Portugal,
2. Instituto de Telecomunicações, DEEC, IST, Av. Rovisco Pais, 1049-001, Lisboa, Portugal
E-mails. joseper@est.ips.pt, poctav@alfa.ist.utl.pt, psgirao@alfa.ist.utl.pt, hgramos@alfa.ist.utl.pt

Abstract: *A low-cost absorbance meter for dissolved compounds identification and concentration evaluation is proposed. The main elements of the system are a white light source and a set of three colored light-to-voltage converters. The system includes auto-calibration capabilities and compensates spectral sensitivity variation of the optical source and detectors. A neural network-processing scheme is used to identify dissolved compounds and evaluate the correspondent concentrations.*

Keywords: *absorbance measurement, error compensation, neural networks.*

1. INTRODUCTION

Absorbance measurements have crucial importance in all chemical processes where concentration measurement is required and, particularly, when variation of concentration over time is needed as a direct measurement of a chemical reaction velocity. For a given compound and length of the light path in the medium, absorbance has a linear dependence on concentration (Beer's law)[1].

Spectrometers are generically used for absorbance, transmittance and concentration measurements but the cost of these instruments is typically high. The present paper presents a low-cost solution with enough accuracy for industrial applications with low accuracy requirements. The solution presented takes advantage of low-cost hardware components and of signal processing performed by a programmable microcontroller (PIC 16F877)[2] and pays particular attention to several system's errors minimization like: optical power source variations, ambient lighting noise and analogue-to-digital converter errors. Auto-calibration capabilities [3] and a ratiometric measurement method are used to cancel common errors of the measurement chain.

Main applications of the measurement system are in the classification and concentration evaluation of solutions, and in the interpolation of absorbance measurements.. Other potential application of the system is color measurement of the water that together with turbidity measurements [4][5] can deliver important parameters for water quality evaluation.

2. SYSTEM DESCRIPTION

Figure 1 represents the measurement system block diagram that includes, besides the optical part, a conditioning circuit with a programmable gain amplifier (PGA), a programmable microcontroller (PIC) and a display to represent measured values.

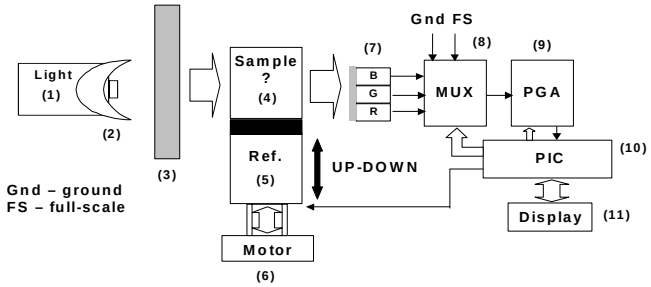

Fig. 1. Measurement system block diagram: (1) white light source; (2) parabolic reflector; (3) optical diffuser and focusing lenses; (4) solution to be measured; (5) reference medium; (6) up-down positioning motor; (7) colored light-to-voltage converters (blue, green and red); (8) analog multiplexer; (9) programmable gain amplifier; (10) programmable interface controller; (11) display.

A two-stage measurement scheme is considered in order to overcome common errors of the measurement system. In the first stage, the sample solution is placed in front of the light beam and three colored light-to-voltage converters measure the transmitted power. In a second stage, the reference, or blank, solution is placed in front of the light beam and the transmitted

(incident) optical power is measured. Vacuum, air, distilled water or any standard solution, with the same composition of the sample solution (comparative measurements), can be used as reference. The solution to be measured and the reference medium are placed in standard 10 mm path-length cells. An additional calibration procedure can be considered if a standard solution is available. In this case, the relative sensitivities of the optical detectors can be evaluated and the correspondent calibration coefficients used for error compensation. These features represent an auto-calibration capability of the measurement system that improves its accuracy.

A. Light Source

The optical source selection, which affects directly the performance of every optoelectronic measurement system, is based on a compromise among the following characteristics: brightness, spectrum bandwidth, size and lifetime. The lamp and reflector chosen have the following main characteristics: 1) lamp - 5.0 V, 0.44 A, 2.2 W, 2.0 candle power, 2750 Kelvin color temperature and 1000 life hours; 2) reflector - parabolic with 0.50" diameter and overall length, 0.189" ream, 0.07" focal distance. Figure 2 represents the optical source spectrum that exhibits a power variation lower than 10 dB in the bandwidth of interest.

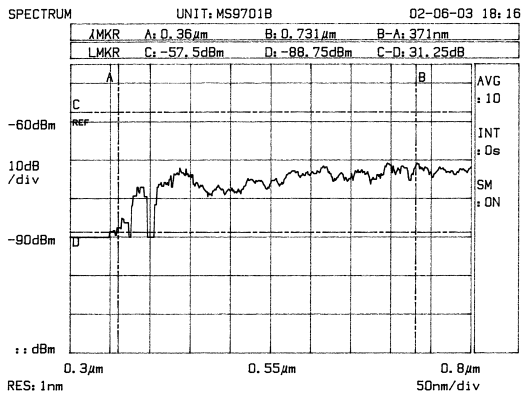

Fig. 2. Optical source spectrum.

B. Detectors

The transmitted light through the solution is detected by a set of three colored light-to-voltage converters. Figure 3 represents the electrical diagram of the selected detectors (TSLB257, TSLG257 and TSLR257). The detectors are high-sensitivity and low-noise light-to-voltage converters that include in a compact 3-leaded plastic package the following main elements: a color filter, a photodiode and a transimpedance amplifier. The output voltage is directly proportional to the filtered light intensity (irradiance), on each photodiode, and the maximum wavelength sensitivities for blue, green and red detectors is 470 nm, 565 nm and 635 nm, respectively. Each device has a transimpedance gain of 320 MΩ, a dark voltage lower than 15 mV and an integrated r.m.s. (root mean square) noise voltage (dc to 1 kHz) lower than 200 μV. Transimpedance amplifier transfer function is given by:

$$G(s) = \frac{V_0(s)}{I_L(s)} = \frac{R}{1+sRC} \tag{1}$$

where V_0 represents the output voltage and I_L the input current that is proportional to the light intensity detected by the photodiode.

Internal RC components assure a time constant of approximately 70 μs, which mean that the cut-off frequency of the low-pass filter is about 2.27 kHz.

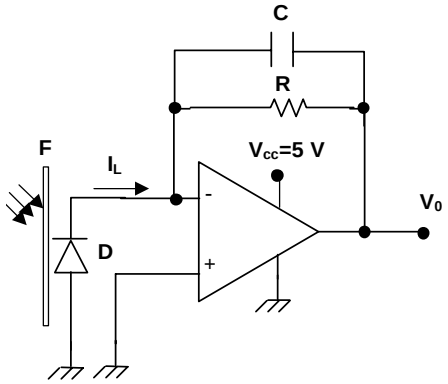

Fig. 3. Electrical diagram of the colored light-to-voltage converter integrated circuit
(F- optical filter, D- photodiode, V_0- output voltage, V_{CC}- unipolar power supply).

The output voltage (V_0) depends mainly on the solution absorbance and on the photodiode spectral responsitivity (Figure 4).

Considering the peak wavelength and the spectral halfwidth of each detector that are equal to: λ_1=470 nm, $\Delta\lambda_{1/2}$=35nm, λ_2=565 nm, $\Delta\lambda_{1/2}$=28nm, λ_3=635 nm, $\Delta\lambda_{1/2}$=25nm, and assuming that the power spectral distribution is approximated by a gaussian function, the output voltage of each photodiode is given by:

$$V_i \cong \int_{\lambda \min_i}^{\lambda \max_i} f_i(\lambda) g(\lambda) d\lambda \tag{2}$$

where f_i represents the spectral responsitivity of each photodiode, g the solution absorbance, and λmin_i and λmax_i are the wavelengths associated with the bandwidth of each photodiode.

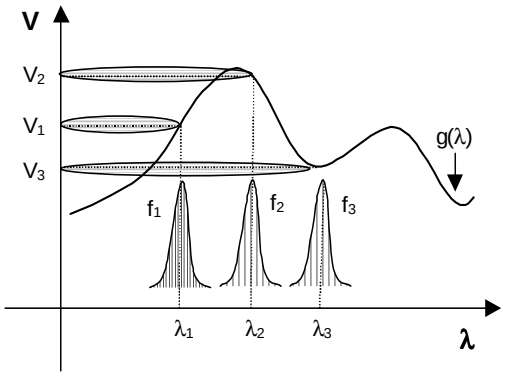

Fig. 4. Detector output voltage as a function of solution absorbance and photodiode spectral responsitivity (f_1- blue detector, f_2- green detector, f_3- red detector).

C. Signal Conditioning

Signal conditioning [6] includes a PGA whose gain is automatically adjusted according to its input voltage level in order to minimize relative errors that are specially important when solution absorbance is high. A ratiometric measurement of incident and transmitted optical powers makes system's accuracy independent of source intensity variations and other common errors of the measurement chain, like temperature and ambient light.

Offset and gain errors of PIC's analog-to-digital converter (ADC) are also cancelled by using ground and full-scale (FS) amplitude measurements.

Figure 5 represents the schematic diagram of the conditioning circuit that includes an instrumentation amplifier (AD524) whose gains of 10-100-1000 are automatically selected by the PIC.

If V_M and V_R represent the voltages that come from the sample solution and from the reference medium, the absorbance for a given wavelength (λ) is given by:

$$A(\lambda) = \log_{10}\left(\frac{P_0}{P}\right) = \log_{10}\left(\frac{V_R/G_R}{V_M/G_M}\right) \qquad (3)$$

where P_0 is the optical incident power, P is the optical transmitted power through the sample solution, G_M and G_R represent the selected gain for sample and reference medium measurements, respectively.

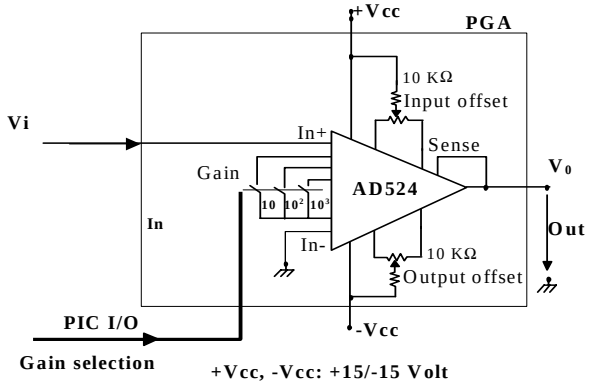

Fig. 5. PGA conditioning circuit (AD524-instrumentation amplifier with selectable gain).

For transmittance measurements, the output voltages from the light converters are acquired and the ratio between transmitted and incident power is computed to provide the transmittance measurement. In this case, the transmittance for a given wavelength (λ) is given by:

$$T(\lambda) = \left(\frac{P}{P_0}\right) = 10^{-abc} = \left(\frac{V_M/G_M}{V_R/G_R}\right) \qquad (4)$$

where a represents the absortivity of the dissolved compound, b the length of the absorption cell (10 mm), c the compound concentration and the others variables have the meanings previously defined.

3. ANN PROCESSING

Signal processing is required to extract the required information from sensors output voltages. Considering the typical non-linear response of the detectors (Figure 4) a neural processing structure [7-9] with three neural networks is considered: one network is used to classify the solution (NN classif), another is used to obtain the tested solution concentration (NN conc.) and the third is used to obtain the absorbance behavior of the tested solution for different wavelenghts (NN abs) (Figure 6). The structure implemented exhibits a good performance even when training of the individual networks uses low size data sets [10].

Besides the general advantages of the usage of neural networks [11], in this particular case their capacity to pattern recognition is used to identify the type of the solution and their capacity to model non-linear systems behavior (Figure 7) is used to interpolate and extrapolate absorbance measurement data.

A. Solution Classification (Pattern Recognition)

As mentioned before, one of the objectives of the measuring system is to allow the classification of solutions based on their absorbance at three different wavelengths (pattern recognition).

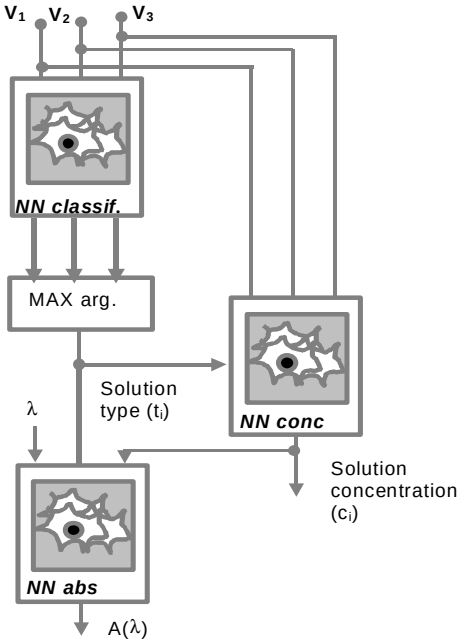

Fig. 6. NN processing structure.

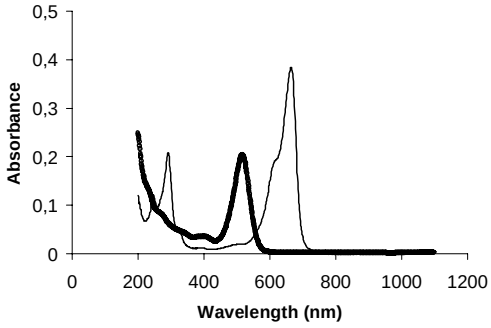

Fig. 7. Absorbance results of methylene blue (normal line) and eosin blueish (bold line) solutions with concentrations equal to 5E-6 M.

To exemplify let us consider that the solution to classify belongs to a universe of three solution types (e.g.. methylene blue, eosin blueish and eosin yellowish), as depicted in Figure 6 (NN classif). Then, a three input, three-output multiplayer perceptron NN can be used. Referring to the training set, it includes the normalized values of the acquired voltage of TSLB257 (blue sensor), TSLG257 (green sensor) and TSLR257 (red sensor) for the three detectors and for different concentrations of each solution (5E-5 M, 1E-6 M, 1E-7 M, 1E-8 M). Thus, for the NN classif, the input matrix of the training set is expressed by light sensor delivered voltages and the output matrix is expressed by the solution type identified by binary sequence with a single 1 value. The NN target matrix is then expressed by:

$$T_{classif} = \begin{bmatrix} 1 & 0 & 0 \\ 0 & 1 & 0 \\ 0 & 0 & 1 \end{bmatrix} \quad (5)$$

The used NN classif characteristics are: input neurons: 3, hidden neurons: 5 tansignoid, output neurons: 3 linear. The training stop condition is $SSE_{STOP}<0.1$.

The obtained NN output values are applied to MAX arg block that selects the type of solution based on the maximum value of the NN output vector. Thus, considering the NN classif test vector $\mathbf{V_t}=[v_1\ v_2\ v_3]^T$, and the corresponding NN output vector $\mathbf{O_t}=[t_1\ t_2\ t_3]^T$ the solution identification is based on the following relations:

$$\begin{aligned} &\text{solution 1} \quad \text{if} \quad t_1 = \max_{i=1\ldots3}(t_i)\ .\text{and.}\ |t_1 - 1| < \delta \\ &\text{solution 2} \quad \text{if} \quad t_2 = \max_{i=1\ldots3}(t_i)\ .\text{and.}\ |t_2 - 1| < \delta \\ &\text{solution 3} \quad \text{if} \quad t_3 = \max_{i=1\ldots3}(t_i)\ .\text{and.}\ |t_3 - 1| < \delta \end{aligned} \quad (6)$$

where $\delta=[0;0.5]$ represents the identification threshold .

B. Concentration Evaluation

For concentration evaluation a three layers perceptron neural network is also used. The hidden layer neurons have also tansignoid activation functions and the dependence between the number of hidden neurons and the NN performance is presented in Figure 8.

Analyzing the figure it is possible to conclude that the optimal solution is 14 tansignoid neurons in the hidden layer. The error in this case is smaller than 0.05 ppm. As output layer is used one linear neuron that delivers the concentration information. The set used to train the network is the same used to train NN classif. After the training phase, the NN is tested using different solutions with concentrations included in the [0.01, 50] ppm interval.

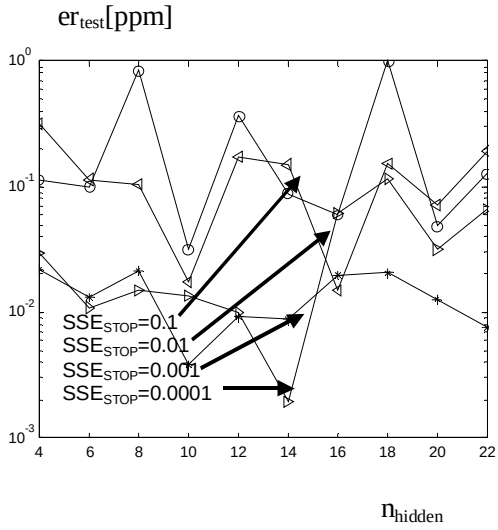

Fig. 8. The evolution of NN conc test error versus the SSE training stop condition and the number of neurons on the hidden layer.

C. Absorbance Characteristic Evaluation

The interpolation and extrapolation capabilities of neural networks are used to obtain the absorbance values for the different type of solutions of a given concentration. Training data is obtained using a spectrometer UNICAM 5625 series. The NN used (NN abs) has three inputs and one output perceptron. The number of hidden tansignoid neurons is equal to 10 and the training stop condition is expressed by SSE_{STOP}<1E-4.

IV. RESULTS

A. Solution Classification

Several results regarding solution classification are presented in Figure 9 under the form of detection rate (DR) versus threshold value, δ. The results are experimental and obtained for different test sets. The detection rate (DR) is calculated using the following formula:

$$DR[\%] = \mathrm{abs}\left(1 - \frac{n_{real} - n_{detect}}{n_{real}}\right) \cdot 100 \qquad (7)$$

where n_{real} is the number of values for classification and n_{detect} is the number of correct classifications.

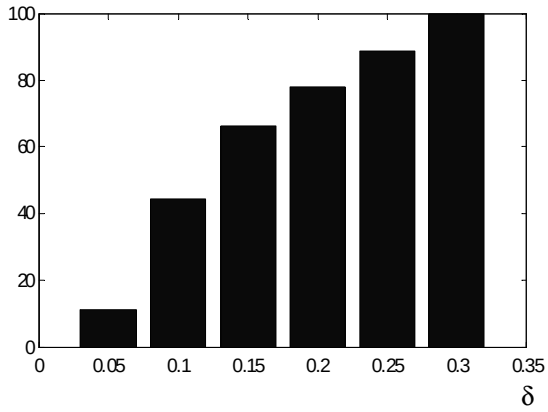

Fig. 9. Solution classification: DR versus δ.

Considering previous results a threshold of 0.3 is used in order to maximize detection rate.

B. Concentration Evaluation

As shown in Figure 8 for a particular type of solution (eosin blueish), for the selected number of hidden neurons (14) and stop condition (1E-4), the error in concentration evaluation using the measuring system is 2×10^{-3} ppm in the worst case. This value corresponds to relative errors much smaller than 1%. Thus, it is fairly safe to say that the system allows concentration measurements with 1% inaccuracy.

C. Absorbance Evaluation

Considering that the solution type and concentration are known, Beer's law establishes, for low solution concentrations (c<1E-2 M), a linear dependence between absorbance and concentration:

$$A(\lambda) = \varepsilon(\lambda)bc \qquad (8)$$

where A is the absorbance, ε the absortivity of the dissolved compound, b the optical cell length and c solution's concentration. Theoreticaly in a logarithmic scale, the curves of absorbance for different concentrations can be obtained by translation. However practical results shows significant deviations from Beer's law even for low concentrations. Figure 10 represents absorbances results for an eosin blueish solution with the following concentrations: S1 - 5.10^{-5} M; S2 - 10^{-6} M; S3 - 10^{-7} M; S4 - 10^{-8} M.

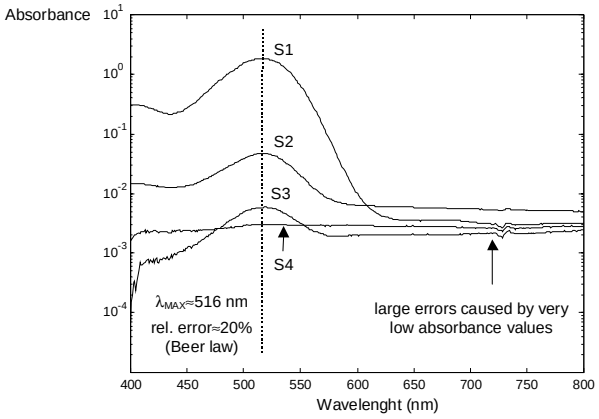

Fig. 10. Beer's law deviations: absorbance for different values of concentrations.

To test the interpolation capabilities of the neural network (NN abs) in foreseeing the absorbance results of a solution of a given concentration, two solutions of eosin blueish with different concentrations values are considered, C1=5E-5 M and C2=5E-6 M, and the correspondent spectrometer data is used to train the NN abs. After the training phase, the NN abs is tested using eosin blueish solution characterized by C3=(C1+C2)/2. The normalized absorbance evolution obtained in the test phase for the three concentrations is shown in Figure 11.

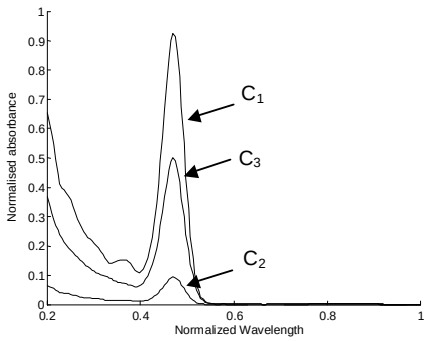

Fig.11. The normalized absorbance graph obtained on the NN abs test phase.

Referring to the results obtained for C3 using the NN abs, the absorbance evaluation relative error is calculated using data obtained with the spectrometer. Error results are presented in Figure 12 that reveals a relative errors smaller than 3%. It should be noted that since the absorvity is a function of the wavelength, it is only possible to obtain the curve of C3 from curves relative to C1 and C2 if that dependence in known.

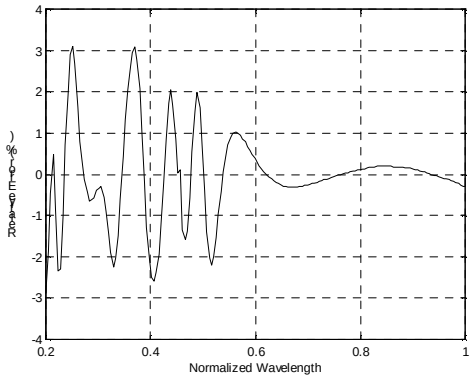

Fig.12. The absorbance evaluation relative error for the NN abs and tested eosin blueish solution.

V. CONCLUSION

The paper presents a low-cost solution for absorbance and transmittance measurements. The main characteristics and novelties include auto-calibration capabilities to compensate for incident power variations, external light disturbances, offset and gain ADC errors and sensitivity variation of optical detectors (aging). Ratiometric measurements and a post-processing software, based on artificial neural networks, improves system's accuracy and provides identification of sample compounds and correspondent concentrations.

In what solution classification is concerned, the proposed measuring system produces total success provided that a convenient design is used. In concentration and absorbance evaluation, the errors obtained with the system are smaller than 1% and 3%, respectively, values quite acceptable for industrial applications requiring medium accuracy.

ACKNOWLEDGEMENTS

This work was supported both by Portuguese Science and Technology Foundation PRAXIS XXI program FCT/BPD/2203/99 and by Project FCT PNAT/1999/EEI/15052. These supports are gratefully acknowledged. We also would like to thank the Departamento de Sistemas e Informática da ESTSetúbal, IPS, for their important technical support.

REFERENCES

[1] D. Skoog, F.J. Holler, T.A. Nieman, Principles of Instrumental Analysis, 5th edition, Saunders College Publishing, 1998.

[2] John B. Peatman, Design with PIC Microcontrollers, Prentice Hall, 1998.

[3] Frank van der Goes, Gerard Meijer, "A Simple Accurate Bridge-Transducer Interface with Continuous Autocalibration", IEEE Trans. Instrum. Meas., Vol. 46, No.3, pp. 704-710, June 1997.

[4] O. Postolache, M. Pereira, P. Girão, "An Intelligent Turbidity and Temperature Sensing Unit for Water Quality Assessment", Proc. of 2002 IEEE Canadian Conference on Electrical & Computer Engineering, Winnipeg, Canada, 12-15 May 2002, pp.494-499.

[5] O. Postolache, P. Girão, M. Pereira, H. Ramos, An IR Turbidity Sensor: Design and Application, Proc. of IEEE Instrumentation and Measurement Technology Conference, Anchorage, AK, USA, 21-23 May 2002, pp.535-540.

[6] Daniel H. Sheingold, Transducer Interfacing Handbook, Analog Devices Inc., 1981.

[7] R. Rojas, Neural Networks – A Systematic Introduction, Springer Berlin Heidelberg, New York, 1996.

[8] S. Haykin, Neural Networks - A Comprehensive Foundation, Prentice Hall, 1999.

[9] C. Jain, N. M. Martin, Fusion of Neural Networks, Fuzzy Seta, and Genetic Algorithms - Industrial Applcations, CRC Press LLC, 1998.

[10] J.M. Dias Pereira, P. Silva Girão, O. Postolache, "Fitting Transducer Characteristics to Measured Data", IEEE Instrumentation & Measurement Magazine, Vol.4, No.4, pp. 26-39, Dec. 2001.

[11] A. Bernieri, G. Betta, A. Pietrosanto and C. Sansone "A neural network approach to instrument fault detection and isolation" IEEE Trans.Instr. Meas., vol. 44, pp.747-750, June 1997.

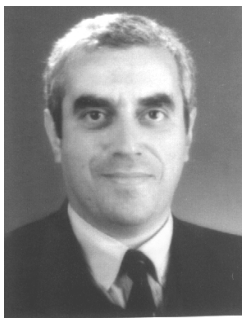

J.M. Dias Pereira *(M'02) received his degree in Electrical Engineering from the Instituto Superior Técnico (IST) of the Technical University of Lisbon (UTL) in 1982. He worked for eight years for Portugal Telecom in digital switching and transmission systems. In 1992, he returned to teaching as Assistant Professor in Escola Superior de Tecnologia of Instituto Politécnico de Setúbal, where he is, at present, a Coordinator Professor. In 1995, he received the MSc degree and in 1999 the PhD degree in Electrical Engineering and Computer Science from IST. His main research interests are in the instrumentation and measurements areas.*

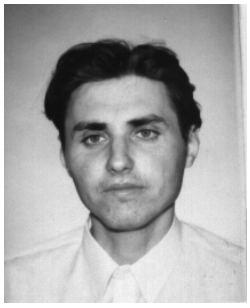

Octavian Postolache *(M'99) was born in Piatra Neamt, Romania, on July 29, 1967. He received the electrical engineering diploma from Technical University of Iasi, Faculty of Electrical Engineering in 1992. In 1992, he joined the Faculty of Electrical Engineering Iasi, Department of Electrical Measurements as an Assistant Professor where he is currently Aux. Prof.. In the last two years he develop a research activity on Instituto Superior Tecnico of Lisbon. His main research interests concern on intelligent sensor, laser systems and neural processing in automated measurement systems.*

P.M.B. ***Silva Girão*** *(M'00, SM'01) was born in Lisbon, Portugal, on February 27, 1952. He received the Ph.D. degree in electrical engineering from the Instituto Superior Técnico of the Technical University of Lisbon (IST/UTL) in 1988. In 1975, he joined the Department of Electrical Engineering at IST/UTL, first as an Assistant Professor and, since 1988, as an Associate Professor. His main research interests concern instrumentation, measurement techniques as well as physical and mathematical problems involved in modelling magnetic materials. Metrology, quality and electromagnetic compatibility are also areas of regular activity mainly as auditor for the Portuguese Institute for Quality (IPQ).*

Helena Maria G. Ramos *was born in Lisbon, Portugal, on October 18, 1957. She received the M.Sc. and Ph.D. degrees in electrical engineering from the Instituto Superior Técnico of the Technical University of Lisbon (IST/UTL), in 1987 and 1995 respectively. In 1981, she joined the Department of Electrical Engineering at IST/UTL, first as Assistant and, since 1995, as a Professor. Her main research interests are in the area of instrumentation and measurement techniques.*